EFFECT OF HEAT TREATMENT TEMPERATURE ON THE MICROSTRUCTURE, WEAR AND FRICTION OF Ni–Nb–V ALLOYED MANGANESE STEEL

Souad Ayadi and Ali Hadji
Foundry Laboratory, BADJI Mokhtar Annaba University, BP 12, 23000 Annaba, Algeria

Emrullah Hakan Kaleli
Faculty of Mechanical Engineering, Mechanical Engineering Department, YILDIZ Technical University, Yıldız, 34349 Besiktas, Istanbul, Turkey

Copyright © 2024 American Foundry Society
https://doi.org/10.1007/s40962-024-01363-z

Abstract

The focus of this work is the effect of heat treatment temperature upon the microstructure, hardness, wear and friction of high manganese steel produced in an industrial setting. The obtained steels were subjected to two heat treatments, one at 1050 °C and the other at 1100 °C followed by water quenching. The microstructures were characterized by optical microscopy and scanning electron microscopy equipped with an energy-dispersive spectrometer. Rockwell C hardness and Vickers microhardness were also measured. Wear behavior in dry conditions was investigated under a load of 300 N using pin-on-disk method. Tribological behavior in boundary lubricated conditions under a load of 60 N at high temperature (100 °C) was studied using a custom-made reciprocating tribometer by measuring the mass loss and the friction coefficient. A 5W-40 engine oil was used as lubricant. Atomic force microscopy (AFM) analysis and roughness 2D and 3D of the tested samples were measured. The obtained results showed that in the as-cast state, the added elements favored the formation of simple or complex inter- and intragranular carbides. In the heat-treated state, the microstructure of the examined steels consists of retained austenite, martensite and precipitates. Increasing of heat treatment temperature increases the rate of the formed martensite. Formation of secondary carbides and increasing of martensite amount led to the improvement of hardness and wear resistance.

Keywords: *manganese steel, heat treatments temperature, microstructure, wear, friction*

Introduction

Manganese steel is one of the ideal materials for impact and wear applications. It is widely used in impact hammers, grinding mill liners, crusher jaws and railroad crossings. Generally, it is a steel which does not have high hardness but it has a high capacity for work hardening during its operation.[1–4]

This steel is particularly promising for the manufacture of parts intended for several industrial applications in an environment dominated by wear.[5,6] However, the austenitic microstructure of this steel gives them a sensitivity to wear which limits their lifespan and imposes additional costs on the user sector.[7,8] For decades, researchers have put a significant effort in order to improve the wear behavior of manganese steel.[9–11] Several surface hardening methods have been proposed, namely the application of thermochemical nitriding treatments, the use of deposits of several millimeters by diffusing the carbides resistant to wear and surface treatment by shot blasting or impact. Mass hardening methods have also been used such as the addition of alloying elements and essentially carbides forming elements.[12–14] In this state, a large quantity of carbides can be formed around the austenitic grains, promoting an improvement in hardness but leading to brittleness of the steel. Application of heat treatments has also been proposed in order to obtain a completely austenitic structure enriched with added elements.[15,16] The austenitic structure in this case can only be obtained after the application of several austenitization treatments followed by high

Received: 01 March 2024 / Accepted: 20 April 2024
Published online: 29 May 2024

Table 1. Chemical Composition of the Studied Steel (wt%)

Steels	Elements (wt %)									
	C	Mn	Si	P	S	Cr	Ni	Nb	V	Fe
HM-NiNbV	0.954	10.36	0.285	0.053	0.005	1.48	1.09	0.193	0.356	Bal.

temperature tempering. These operations are expensive and require an in-depth study of each stage of production and mastery of heat treatments. For this purpose, the application of several heat treatments remains rarely used at the industrial level.

It has been shown that addition of alloying elements coupled with a proper heat treatment process enhances the hardness and the mechanical proprieties of castings. However, this increase based mainly on secondary hardening can result in waste of expensive elements such as V and Nb if heat treatment is inappropriate. Although Nb and V, as carbides forming elements, have multifunctional contribution to improve the proprieties of steels, in the as-cast state, these elements favor the formation of secondary carbides, while in the heat treated stated, these elements improve the hardenability of the steel, which increases the hardness and the wear of the steel.[17,18]

Over the years, Nb and V have proved to be among of the most important alloying elements used to improve the wear and the tribological behavior of the manganese steel.[19] These elements were used with higher contents, which makes the material more expensive and uneconomical.

In this study, Nb and V were added as micro-alloying elements with the aim of improving the usage properties of the studied steel while keeping a lower cost of production. Ni was also added in order to maintain certain ductility of the considered steel to avoid its fragility.

The objective of this study, in addition to the addition of Ni, Nb and V, is to define a heat treatment which gives to the manganese steel the best wear and friction properties.

Experimental Procedures

Melting, Casting and Heat Treatments

In this study, high Mn (HM) steel was investigated. The studied steel is melted using a medium frequency electric arc furnace in an industrial environment. Alloying elements (Ni, Nb and V) were finely crushed and added, after the complete melting, in a well heated ladle. The obtained high manganese steel (alloyed with Ni, Nb and V) were cast in furan resin sand molds to produce cylindrical specimens of 100 mm in length and 20 mm in diameter, from a pouring temperature of 1500 °C. The alloyed steel using in this study was symbolized by HM-NiNbV steel. Table 1 lists the chemical composition, given by atomic emission spectrometry, of the studied alloy.

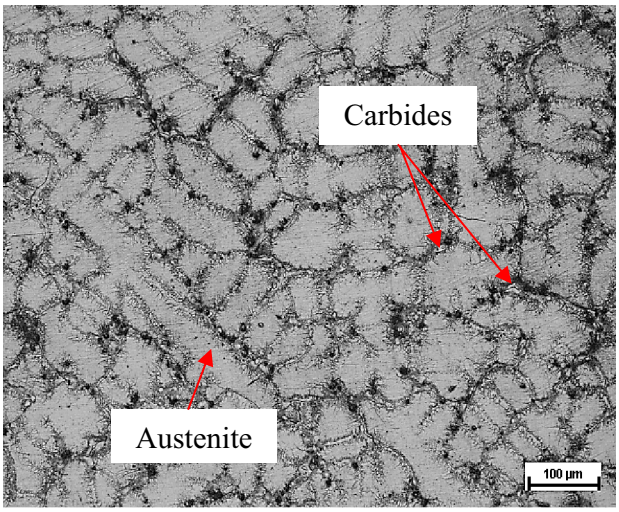

Figure 1. Optical micrographs (X100) in the as-cast state of HM-NiNbV steel.

The heat treatments were carried out in an NABERTHERM brand chambered high temperature furnace. Two heat treatments were applied. The first one consists of heating the specimens at 600, 1020 and 1050 °C for one hour in each temperature with a heating rate of 06 °C/min, followed by rapid water quenching. For the second heat treatment, the samples were heated at 600, 1080 and 1100 °C for one hour in each temperature with a heating rate of 12 °C/min and quenched rapidly in water.

Microstructure Examination

The microstructural observations of the polished and the etched (with 4% Nital) as-cast and heat-treated HM-NiNbV steel was carried out using an optical microscope (OM) and

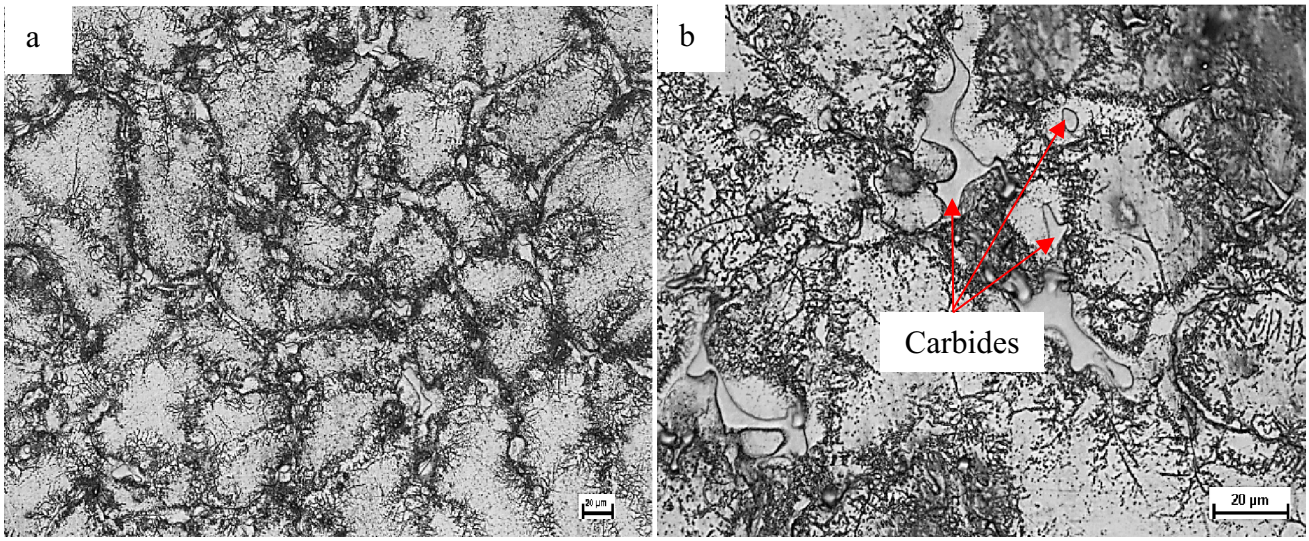

Figure 2. Optical micrographs of formed carbides in the as-cast state. (a) X200, (b) X500.

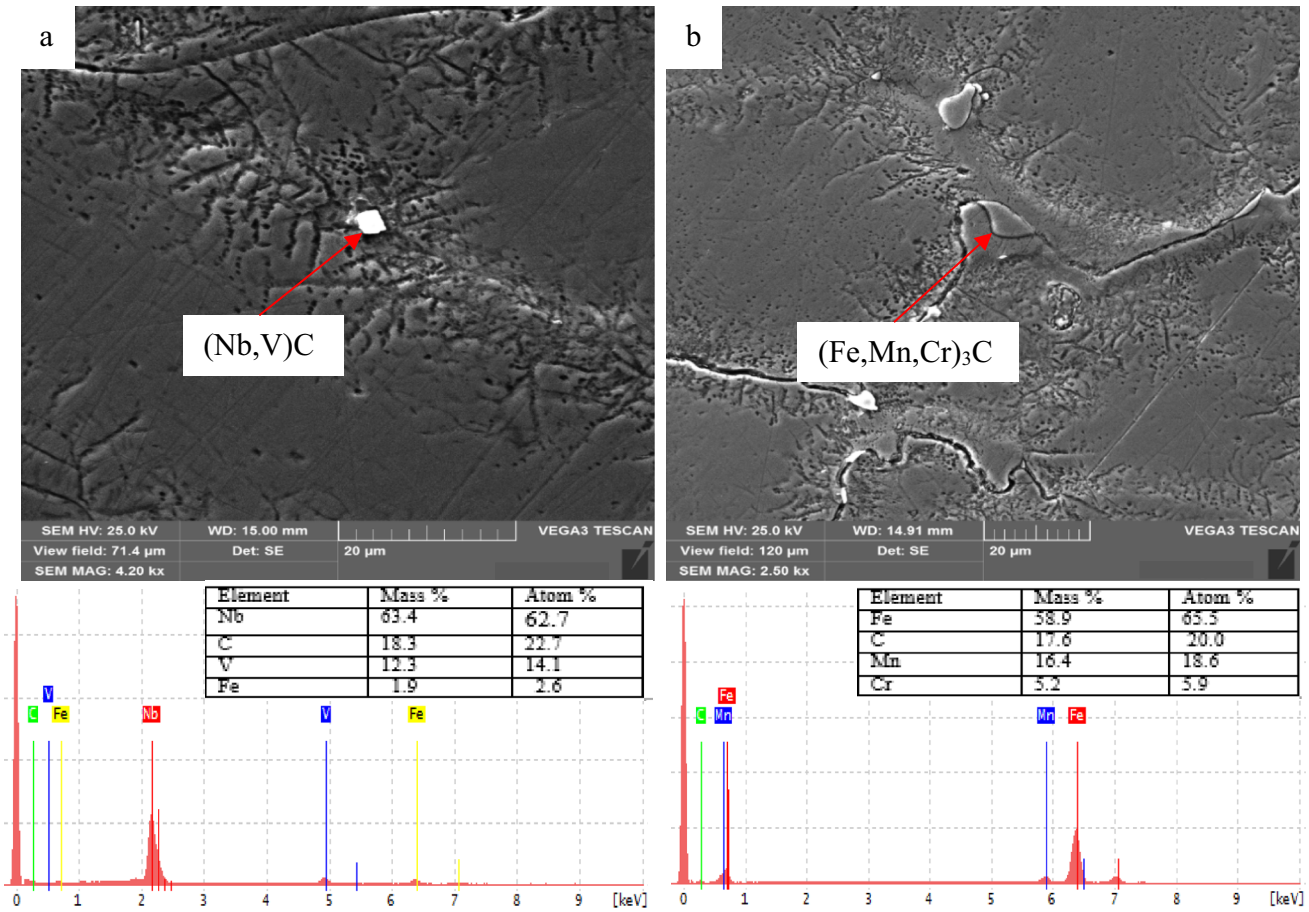

Figure 3. SEM micrographs and EDS analyses of HM-NiNbV steel.

a scanning electron microscope (SEM) equipped with an energy-dispersive spectrometer (EDS).

The phase analysis was carried out using X-ray diffraction (XRD, Rigaku) operating with a Cu-Ka radiation, a $2\theta = 20$ to 100° with a step size of 0.02° and a collection time of 10s. XRD patterns were adjusted using X'Pert HighScore Plus software.

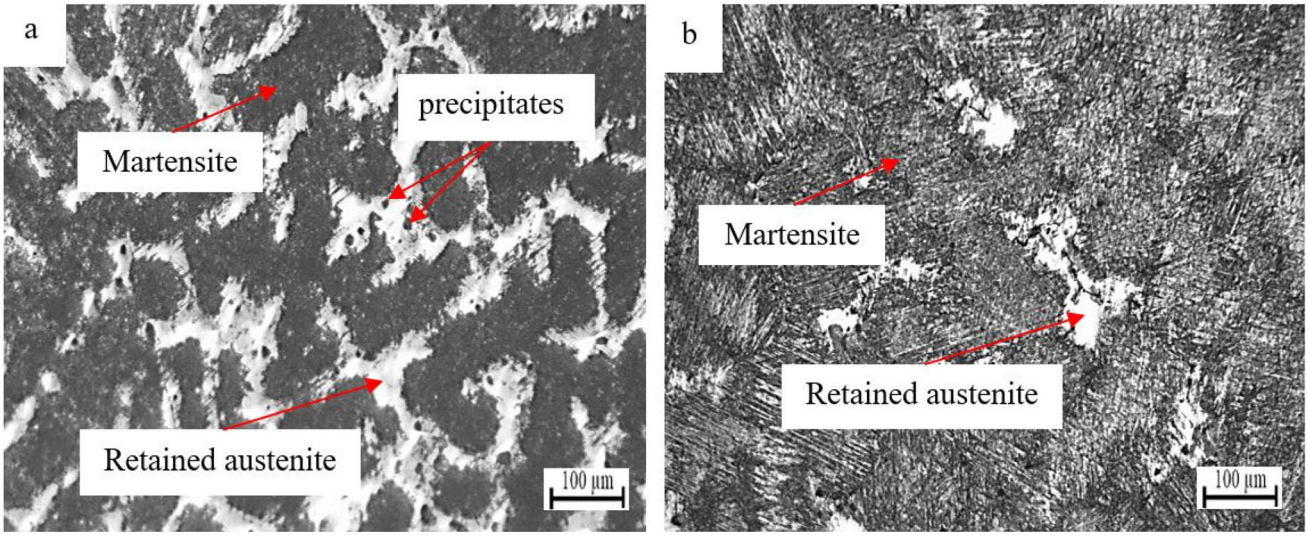

Figure 4. Optical micrographs (X100) of the heat-treated HM-NiNbV steel: at 1050 °C (a) and at 1100 °C (b).

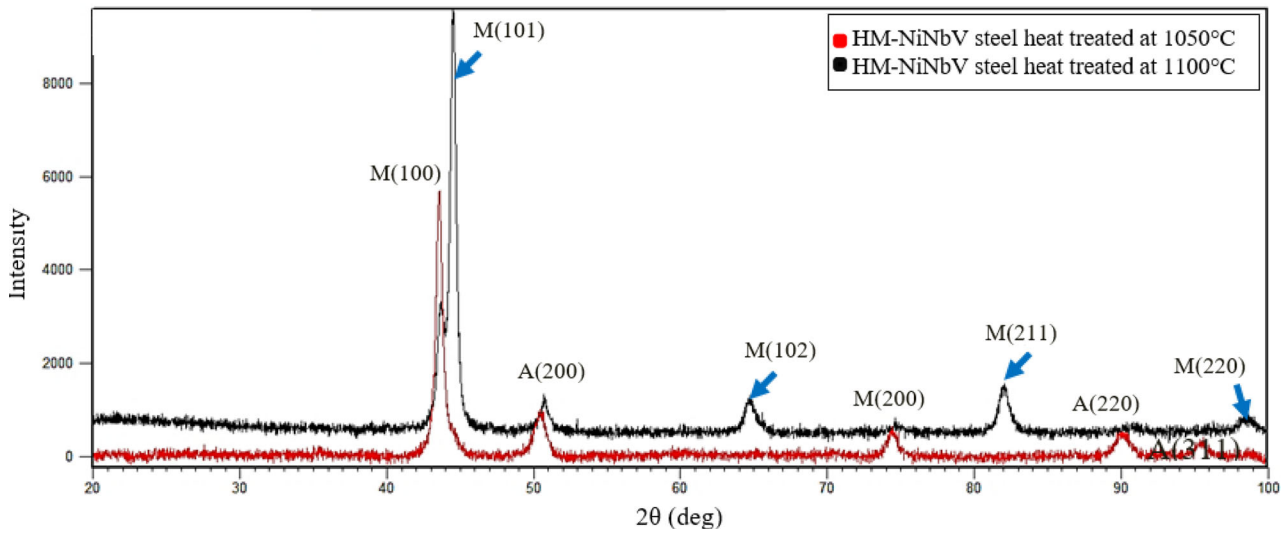

Figure 5. XRD of heat-treated HM-NiNbV steel.

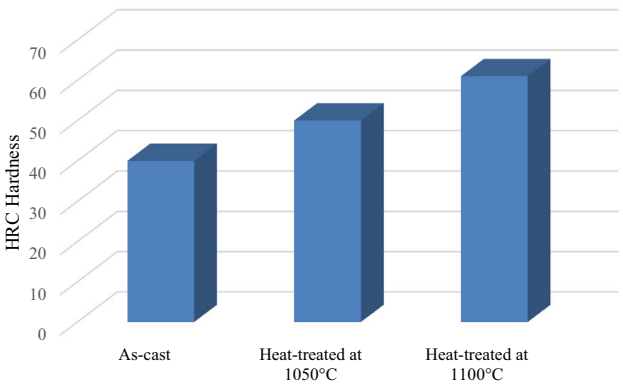

Figure 6. The HRC Hardness of as-cast and heat-treated HM-NiNbV steel.

Hardness, Wear and Tribological Tests

Rockwell C hardness (HRC) was determined according to the ASTM E18 standard under a load of 150 kgf. Vickers microhardness measurements were recorded according to the ASTM E384 standard under a load of 200 gf. Each measurement was repeated three times, using the average value for analysis.

The wear test of the HM-NiNbV steel was conducted according to ASTM G99 in dry conditions against a tungsten carbide disk with a rotation speed of 200 rpm under an applied load of 300 N and a sliding distance of 1000 m. The mass loss of the specimens was measured

Table 2. Microhardness (μHv_{20}) of Different Phases of As-cast and Heat-Treated HM-NiNbV Steel

Cases	As-cast			Heat treated at 1050 °C		Heat treated at 1100 °C	
Phases	Austenite	Carbides		Martensite	Retained austenite	Martensite	Retained austenite
HM-NiNbV steel	418 ± 5	$(Fe, Mn, Cr)_3C$ 1109 ± 20	(Nb, V)C 2312 ± 49	680 ± 6	429 ± 4	766 ± 4	431 ± 5

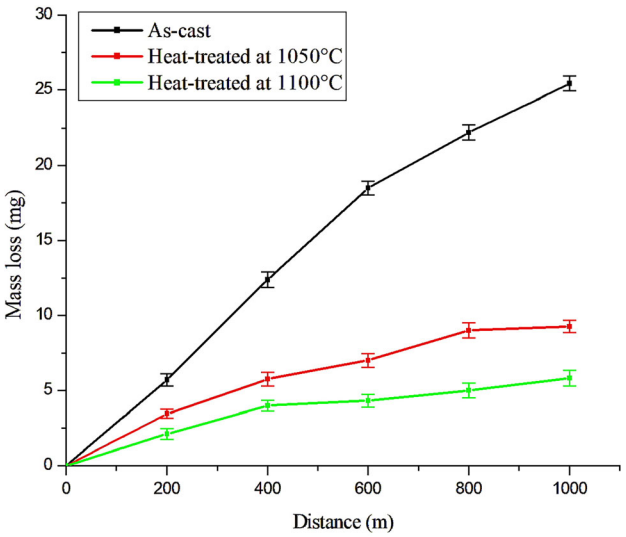

Figure 7. Mass loss of as-cast and heat-treated HM-NiNbV steels.

using an analytical balance with an accuracy of 0.1 mg after each 200 m of test.

The specimens of the HM-NiNbV steel were prepared (polished and cleaned with alcohol) for testing against two types of tribological test to calculate the friction coefficient in different conditions and cover a large area of applications. The first test was performed by using ball-on-disk tribometer under three normal loads 03, 06 and 10 N at sliding speed of 5 cm/s and sliding distance of 100 m. The used ball, with a diameter of 6 mm, was made of 100Cr6 steel. The second tribological test was performed only for the HM-NiNbV steel heat treated at 1100 °C. This test was conducted by using a custom-made reciprocating tribometer at high temperature (100 °C) under a charge of 60N and sliding speed of 0.055 m/s in lubricated conditions against a ball made of 100C6. The used lubricant is a synthetic commercial engine oil (5W-40). The friction coefficient was calculated after two minutes of test. The surfaces morphology of the tested specimen was analyzed

Table 3. Friction Coefficients Values of As-cast and Heat-treated HM-NiNbV Steel

Loads, N	03	06	10
As-cast	0.566	0.570	0.629
Heat treated at 1050 °C	0.610	0.632	0.643
Heat treated at 1100 °C	0.653	0.732	0.747

before and after the test using optical microscopy, scanning electron microscopy (SEM) and atomic force microscopy (AFM).

Results and Discussions

Characterization of Microstructures

The optical micrography of HM-NiNbV (Figure 1) reveals an austenitic matrix with finely distributed secondary carbides. The microstructure of HM-NiNbV steel appears to be relatively fine compared to standard manganese steel. This grain refinement is mostly influenced by the addition of alloying elements, mainly niobium and vanadium. These elements are known as strong carbide-forming elements.[20] They favored the formation of simple or complex carbides of small sizes, with different morphologies (Figure 2) and act negatively on the grain growth, which leads to the formation of a finer structure.

The type and the nature of the formed carbides depend essentially on the added carbide-forming elements. Nb and V are known as strong carbide-forming elements. They form carbides even at low contents (< 1%). The combined addition of these two elements lead to the formation of niobium carbide, vanadium carbides or complexes carbides. Also, Nb is known as a strong carbide -forming element than V. On the other hand, HM-NiNbV steel contains a quantity of V relatively higher than that of Nb,

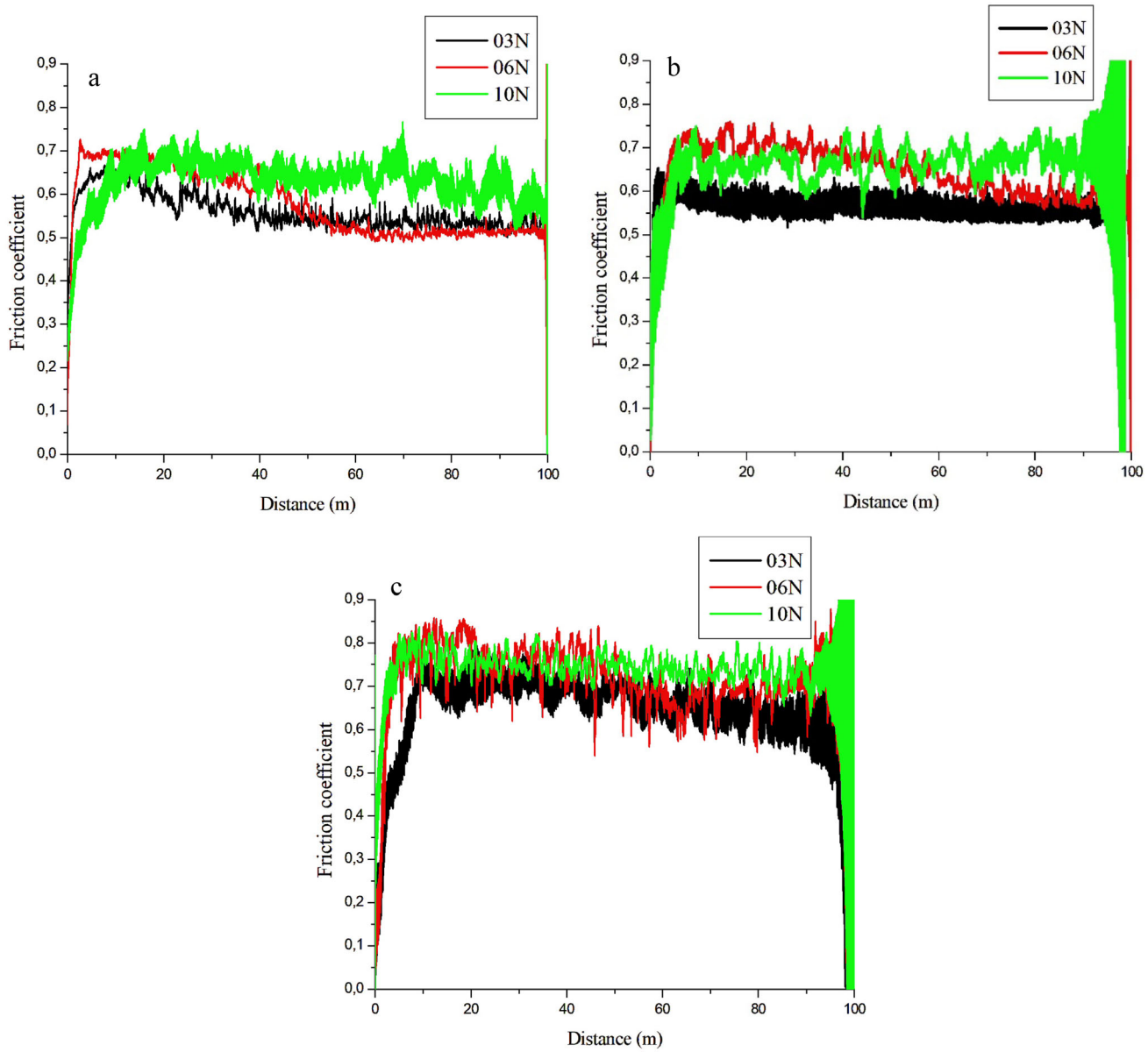

Figure 8. Friction coefficients of HM-NiNbV steel. (a) as-cast, (b) heat treated at 1050 °C and (c) heat treated at 1100 °C.

so the formed carbides are probably Nb-V complex carbides. In order to determine the nature and the type of the formed carbides, EDS analyses were carried out on different areas of HM-NiNbV steel. This analysis (Figure 3a) reveals mainly Nb, V and C pics. Theoretically, Nb and V form MC-type carbides. So, the formed carbide can be (Nb, V)C or (V, Nb)C. According to the obtained Nb pic, the formed carbide is (Nb, V)C.

Another carbide was identified (Figure 3b), it consists of Mn and Cr alloyed cementite. At low content, Cr is distributed between the matrix and the cementite.[21]

After heat treatments (Figure 4), the microstructures of both of the studied HM-NiNbV steel is mainly composed of martensite and retained austenite.[13] Solution treatment of the examined steels at high temperature (1050–1100 °C) followed by water quenching led to the transformation of austenite to martensite. The retained austenite is explained by the incomplete transformation of austenite after the heat treatments under the effect of Ni. This small amount of retained austenite is desirable to preserve certain ductility of the steel after heat treatments, which will serve to improve its service properties and promotes its use in several industries. The amount of the formed martensite changes as a function of the applied heat treatments and the added elements. Based on the obtained microstructures, the amount of martensite shown in the microstructure of HM-NiNbV steel is higher than that of retained austenite for the two heat treatments. This is due to the effect of the added

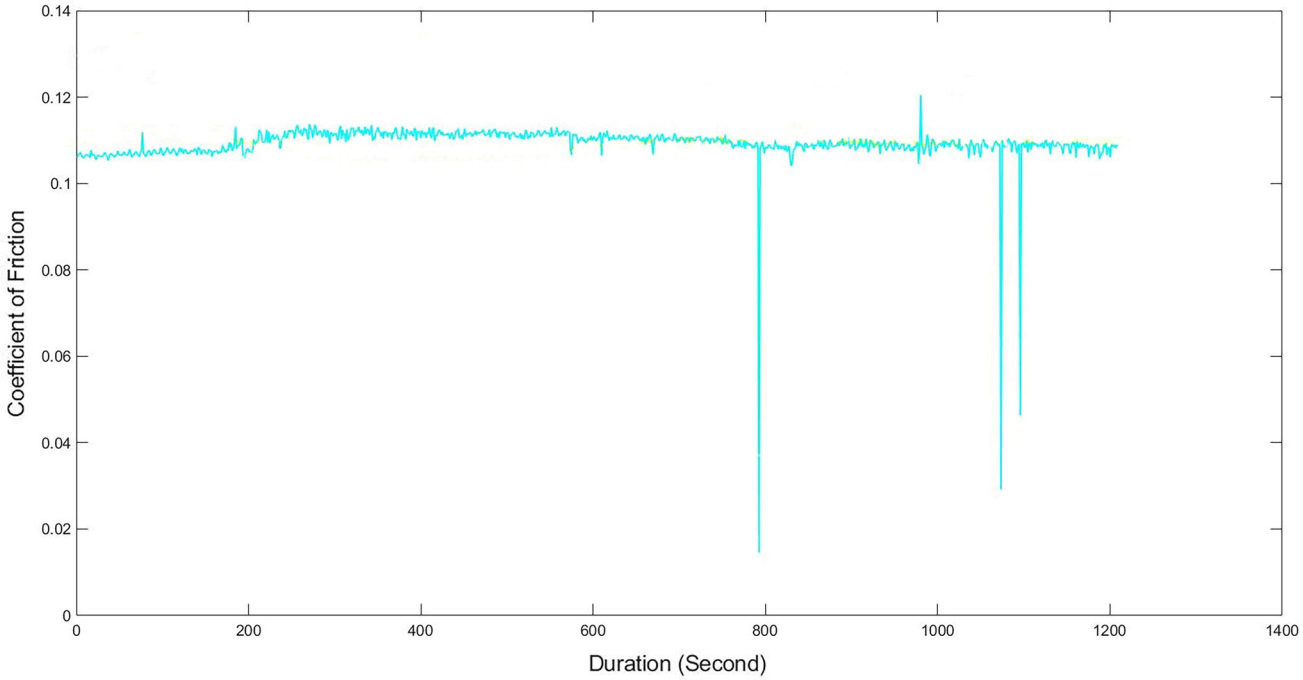

Figure 9. Friction coefficient of HM-NiNbV steel heat treated at 1100 °C at high temperature (100 °C) under a charge of 60N in lubricated conditions.

elements. Addition of Nb and V improves the hardenability of the examined steel and promotes the transformation of austenite to martensite. On the other hand, the amount of the formed martensite increases with increasing in the heat treatment temperature.

A small quantity of precipitates was observed mainly after heat treatments at 1050 °C. These precipitates are very fine and uniformly dispersed in the retained austenite. They can be a product of the incomplete decomposition of as-cast secondary carbides or precipitates formed during dissolution. These precipitates are practically unobservable after heat treatment at 1100 °C. This heat treatment had a greater effect on the dissociation of as-cast secondary carbides and the transformation of austenite to martensite.[5]

In order to confirm the presence of the revealed phases in the heat-treated state, optical observation of the examined steels was followed by XRD analysis (Figure 5). According to Figure 5, martensite (M) and austenite (A) are present for both heat treatments.

XRD patterns reveal that the transformation of austenite to martensite of HM-NiNbV steel heat treated at 1100 °C is much occurred compared to the same steel heat treated at 1050 °C. The martensitic pics in this case are numerous and more intense at 1100 °C. Also, martensite (101), (102), (211) and (200) as an induced phase in HM-NiNbV steel was favored under the combined effect of the added elements and high heat treatment temperature (1100 °C).

Hardness and Microhardness

Figure 6 shows HRC hardness of the as-cast and heat-treated HM-NiNbV steels. As can be seen, HRC hardness of the as-cast HM-NiNbV steels is 40 HRC, which is higher than hardness of standard high manganese steel. In this state, Nb and V improve considerably the hardness by promoting the formation of hard carbides (Nb,V)C. While Ni contributes to raise the matrix hardness. HRC hardness of heat-treated HM-NiNbV steels are 50 HRC after heat treatment at 1050 °C and 61 HRC after heat treatment at 1100 °C, respectively. After heat treatments, the hardness values were found to increase as the heat treatment temperature increase. This is due to the effect of addition of Nb and V, which increases the hardenability of HM-NiNbV steel and favor the formation of large amount of martensite.[15]

Table 2 gives the microhardness measurements of the different existing phases in the as-cast and heat-treated HM-NiNbV steels.

In the as-cast state, austenite of HM-NiNbV steel (418 ± 5 μHv_{20}) is harder than that of standard manganese steel, which is attributed to its enrichment in the added Ni, Nb and V. Ni, as a gamma forming element, is dissolved in the matrix after the solidification of the steel. As for Nb and V, one part participates to the austenite enrichment and the rest forms MC-type carbides. These two elements form with gamma iron a substitutional solid solution allowing to

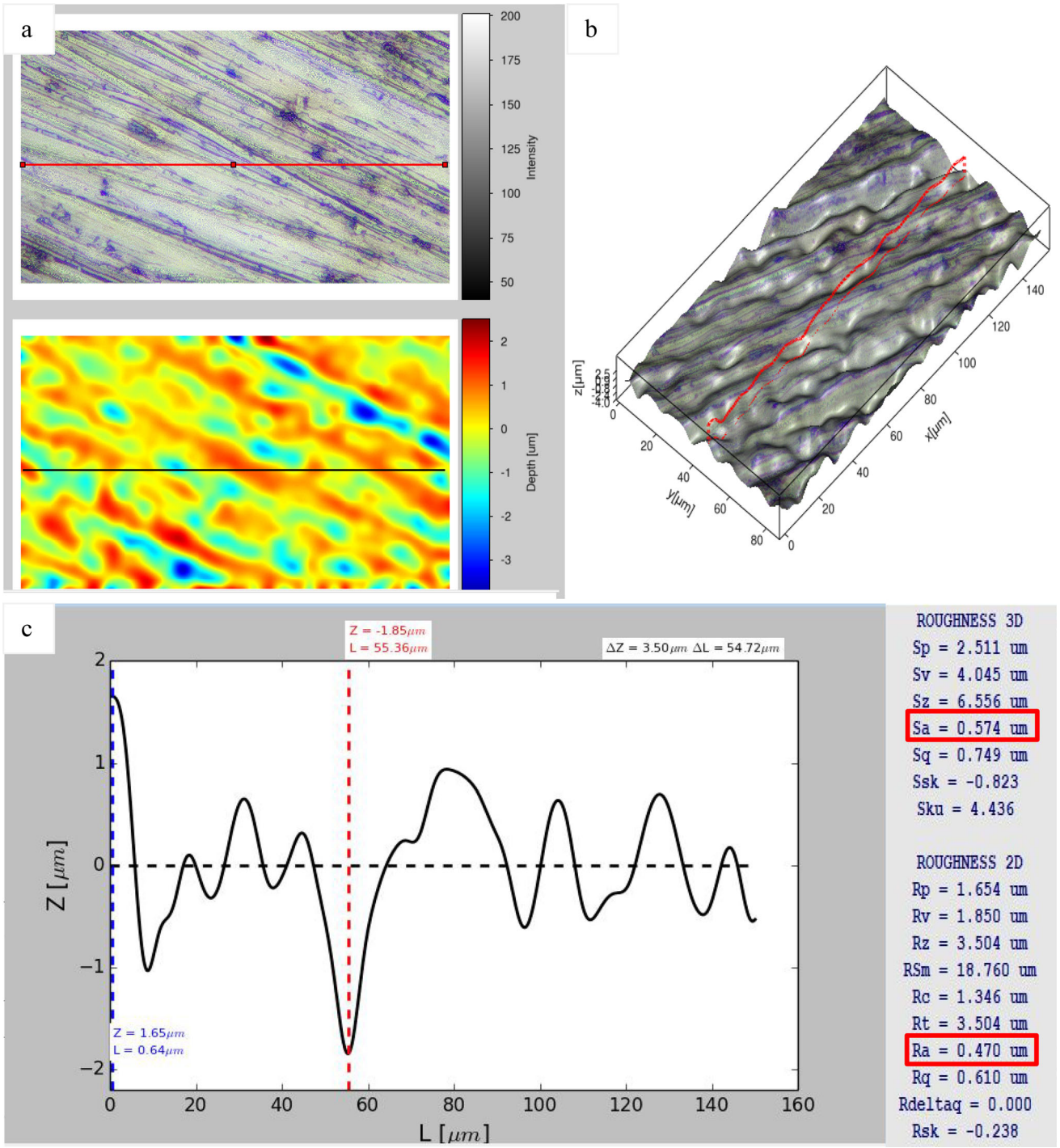

Figure 10. Characteristics of HM-NiNbV steel heat treated at 1100 °C before the tribological test. (a) Optical micrograph 2D, (b) Optical micrographs 3D and (c) Roughness values.

the formation of austenite more compact, which increases the microhardness of this phase.

Nb and V complex carbide shows a higher microhardness (2312 ± 49 μHv_{20}) than alloyed cementite.

In the heat-treated state, martensite and retained austenite of HM-NiNbV steel heat treated at 1100 °C are higher than those of HM-NiNbV steel heat treated at 1050 °C HM steel. Improvement of martensite microhardness is related to the added elements and increasing of heat treatment temperature.

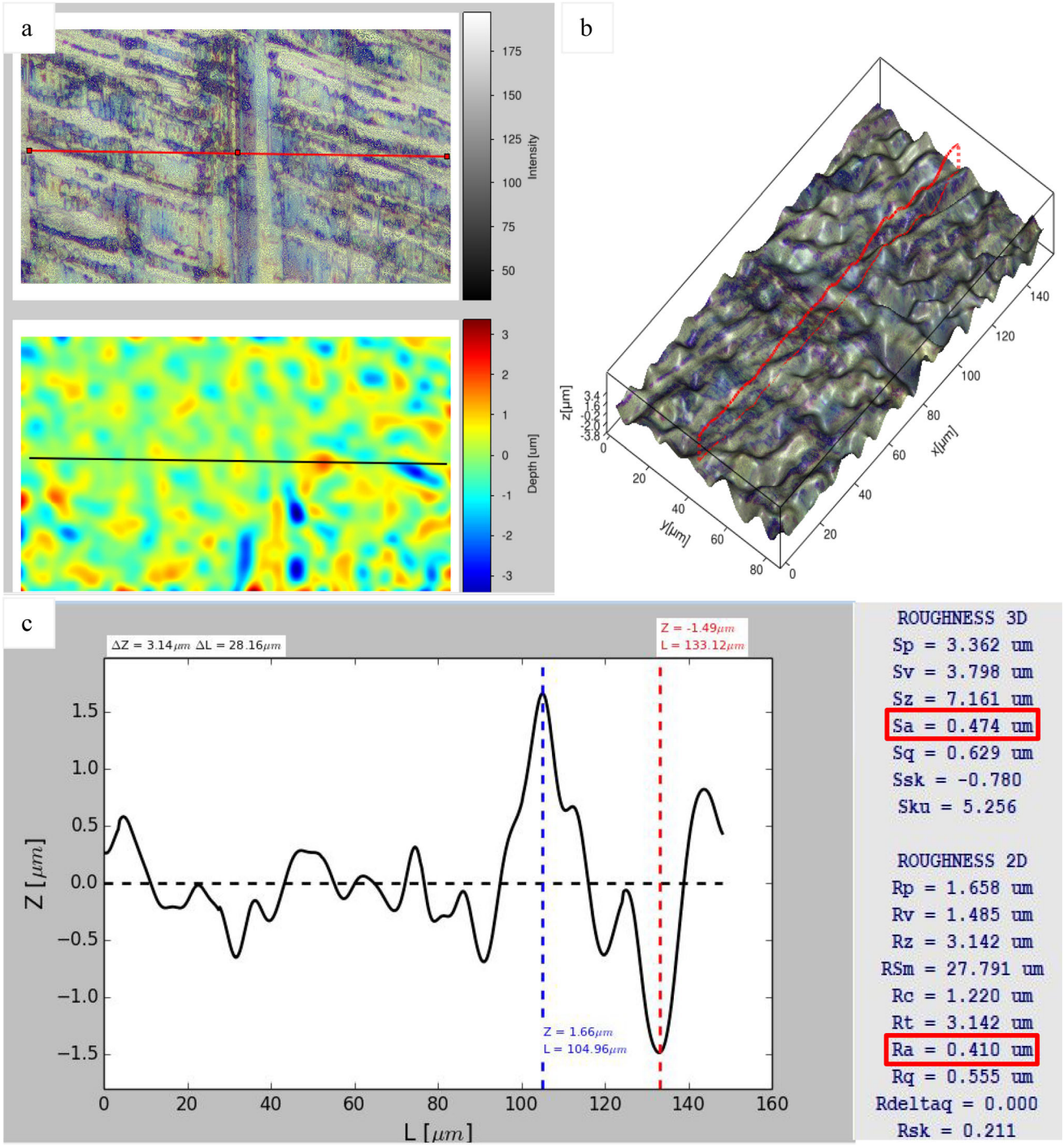

Figure 11. Characteristics of HM-NiNbV steel heat treated at 1100 °C after the tribological test. (a) Optical micrograph 2D, (b) Optical micrographs 3D and (c) Roughness values.

Tribological Behavior

Figure 7 shows the mass loss of as-cast and heat-treated HM-NiNbV steel rubbed against a tungsten carbide (WC) disk under a load of 300 N and a distance of 1000 m. Mass loss of HM-NiNbV steel heat treated at 1100 °C is the lower. Increasing of heat treatment temperature has a considerable effect on wear resistance improvement of HM-NiNbV steel. This is justified by the presence of high amount of martensite, which is known with its high hardness and its high wear resistance.

Friction coefficients of as-cast and heat-treated HM-NiNbV steel under the charges of 03, 06 and 10N in dry conditions at room temperature are given in Table 3 and Figure 8. It is characterized by the Pin-on-Disk test tribometer. The

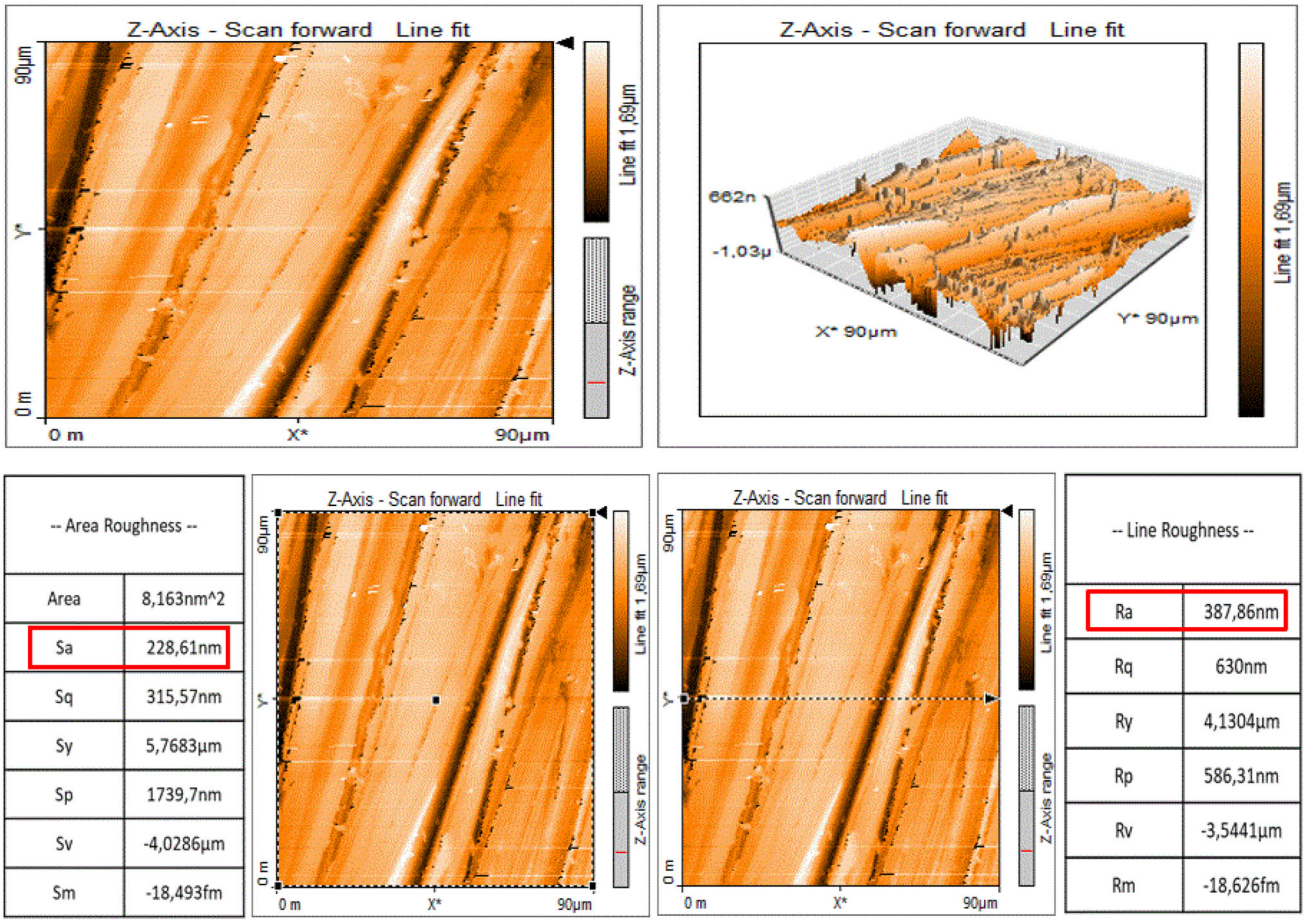

-- Area Roughness --	
Area	8,163nm^2
Sa	228,61nm
Sq	315,57nm
Sy	5,7683µm
Sp	1739,7nm
Sv	-4,0286µm
Sm	-18,493fm

-- Line Roughness --	
Ra	387,86nm
Rq	630nm
Ry	4,1304µm
Rp	586,31nm
Rv	-3,5441µm
Rm	-18,626fm

Figure 12. Atomic force microscopy (AFM) analysis of HM-NiNbV steel heat treated at 1100 °C before the tribological test.

friction coefficient is given by the equation $F = \mu N$, where F = frictional force in Newton, μ = coefficient of friction and N = normal applied force. In this case, the friction coefficient was computed directly during the test.

As reveal in patterns, there is two periods. The first one is at the beginning of testing: a running in period in which the friction coefficients increase with increasing of the applied charges and the second one when the friction coefficient tends to stabilize: a steady state. Increasing of the friction coefficient in the running in period is related to the interaction of the initial asperities of the tested surface and the work hardening occurs in this period. Rubbing between two harder materials (HM-NiNbV steel/ball) led, during the running in period, to a progressive work hardening of the surface of the tested steels and the transformation of austenite to martensite. The stability of the friction coefficient in the steady state explains that there is not an intense microstructural change if the contact surface of the teste steels. According to the obtained results, heat-treated HM-NiNbV steel averages the highest friction coefficient compared to as-cast steel for all applied charges.

Tribological test at high temperature (100 °C), under high charge (60 N) and in lubricated conditions was performed only for HM-NiNbV steel heat treated at 1100 °C. Figure 9 shows the friction coefficient as a function of time (sec) of this steel. The friction coefficient (0.1111) is relatively stable during the test. Intense fluctuations of the friction coefficient are observed from 800 s. This could be due to the existence of a small amount of undissolved carbides. The coefficient of friction measured for this test is lower compared to the tests carried out in dry condition under loads of 03 N, 06 N and 10 N. This is due to the used lubricant. The latter reduces considerably the friction between the ball and the sample, which leads to a remarkable decrease in the coefficient of friction.

In order to study the effect of the friction test on the sample surface, optical, electronic and AFM microstructural analyzes were performed before and after the test. The 2D and 3D roughness of the two surfaces were also measured. Before the test, the sample was mechanically polished (grit 2400).

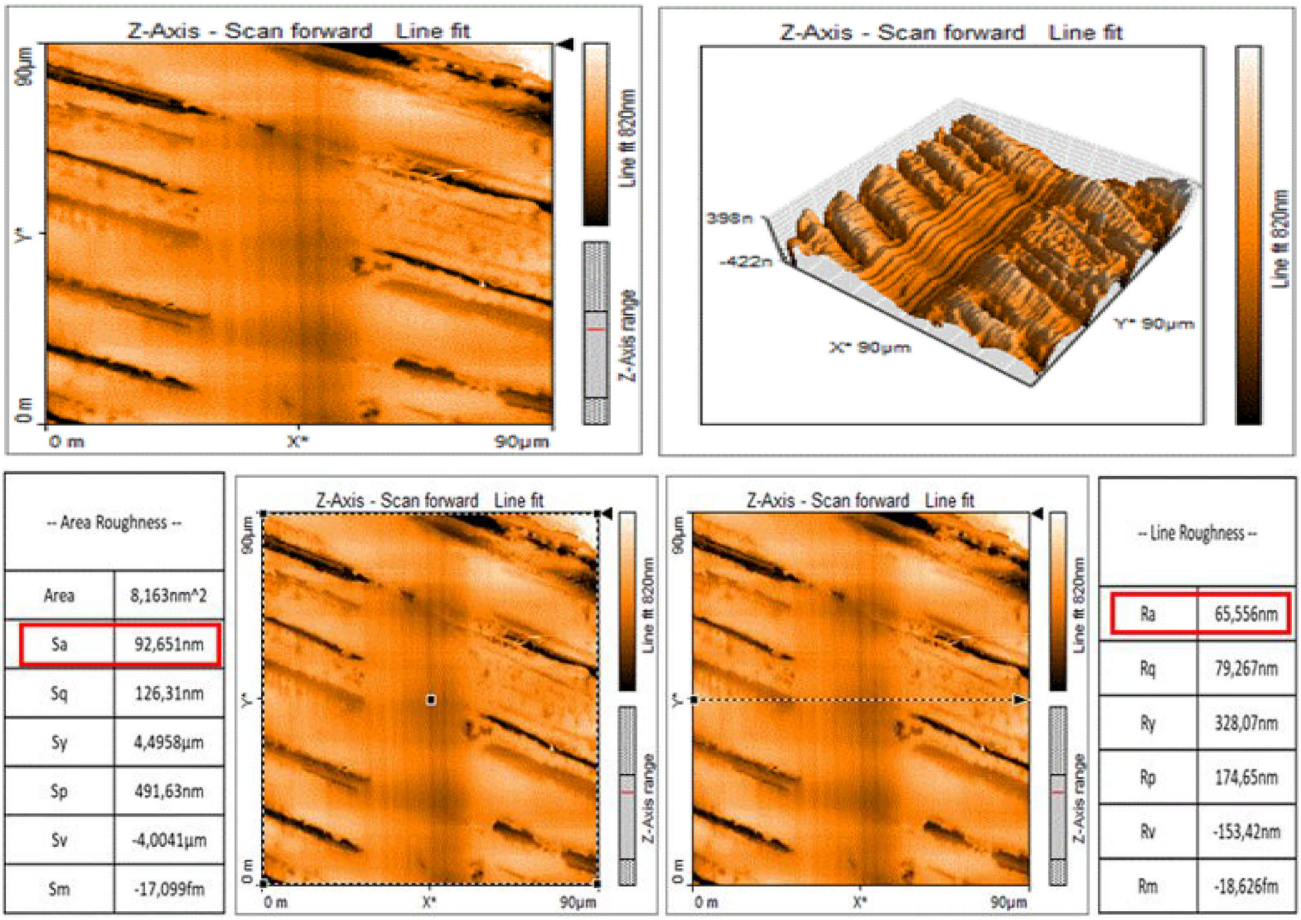

Figure 13. Atomic force microscopy (AFM) analysis of HM-NiNbV steel heat treated at 1100 °C after the tribological test.

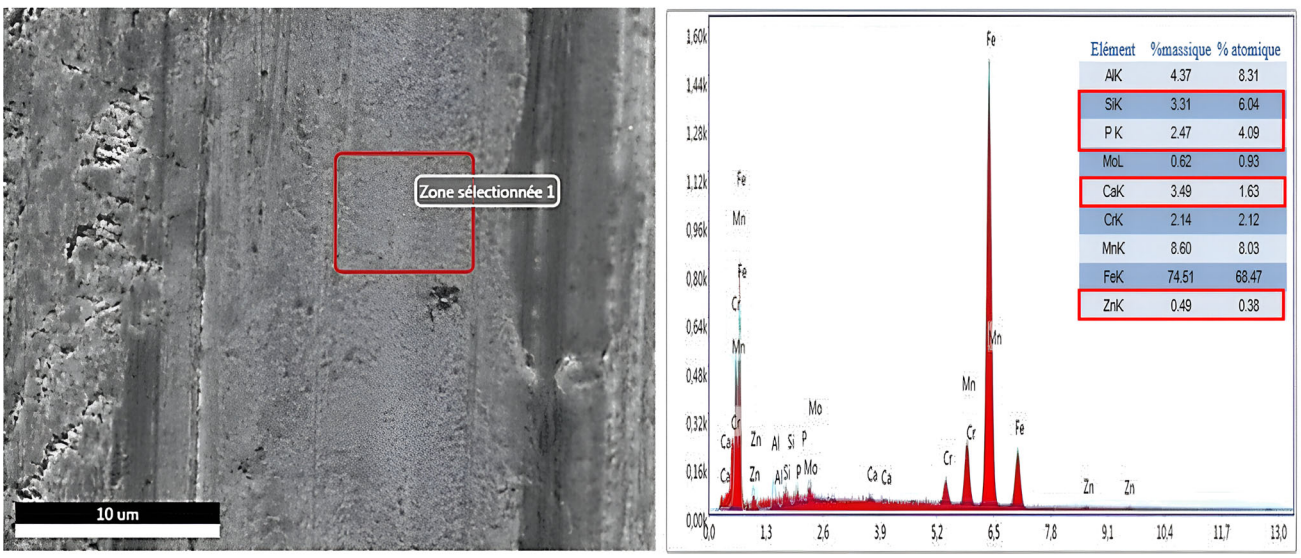

Figure 14. Scanning electron microscopy micrograph and EDS analysis of HM-NiNbV steel heat treated at 1100 °C after the tribological test.

Optical micrographs and the roughness (2D and 3D) of HM-NiNbV steel heat treated at 1100 °C before and after the tribological test are shown in Figure 10. Before the test, the surface sample exhibits the roughness parameters Ra and Sa of 0.470 µm and 0.574 µm, respectively (Figure 10). After the test, a slight decrease in the two parameters was noticed (0.410 µm and 0.474 µm, respectively) (Figure 11). Application of a high load (60 N) at high temperature (100 °C) in the presence of a lubricating oil promotes a finish polishing improving the surface state.

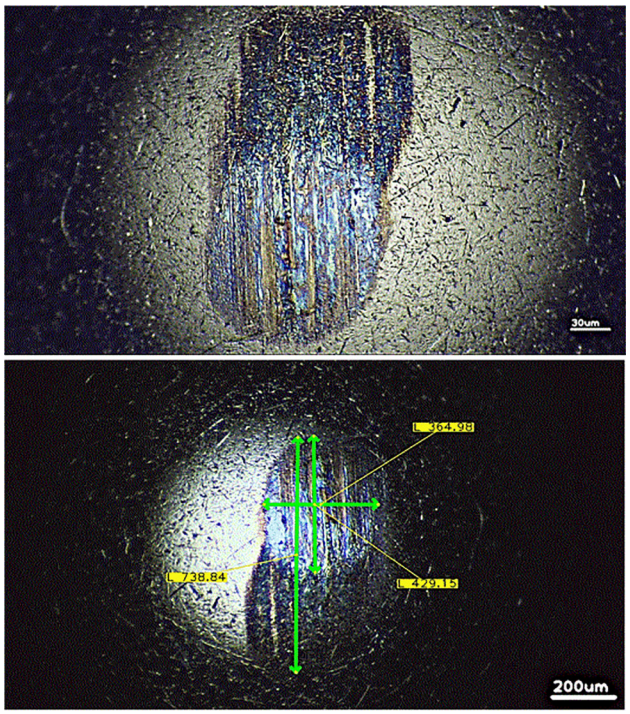

Figure 15. Ball contact surface after the tribological test against HM-NiNbV steel heat treated at 1100 °C.

A nanoscale measurement of the roughness values Ra and Sa of HM-NiNbV steel heat treated at 1100 ° C was performed before and after the tribological test using AFM analysis. The results (Figures 12 and 13) showed that the surface of the sample before the test is rougher than after the test. The roughness values decreased from Ra = 378.86 nm and Sa = 228.61 nm before the test (Figure 12) to Ra = 65.556 nm and Sa = 92.651 nm after the test (Figure 13). This shows a significant improvement in the surface state. As explained in the previous paragraph, the test carried out in the presence of the lubricant allowed a final polishing.

In order to analyze the microstructure of the sample surface after the test, SEM observations and EDS analysis were performed (Figure 14). This analysis showed that the wear track is rich in chemical elements that do not exist in the composition of the steel. These elements are mainly Si, P, Ca and Zn. These are part of the composition of the used lubricant. This shows the formation of a tribofilm on the sample surface during the test, which decreases the wear of the sample and the friction between the latter and the ball.

The ball surface after the tribological test was also analyzed. The optical micrographs and the 2D and 3D roughness are presented in Figure 15.

In order to study the tribological behavior of the ball/sample pair, the ball/plane configuration giving a circular contact area is chosen as the reference configuration for this type of contact. Usually, different geometries can exist. The contact area, in our case, is formed by two ellipses with different lengths of the main axes (429.15 µm and 738.84 µm). This is due to a slight deformation of the ball surface caused by the tested sample (Figure 15). This could be due to a slight increase in the strength of the tested steel during testing.

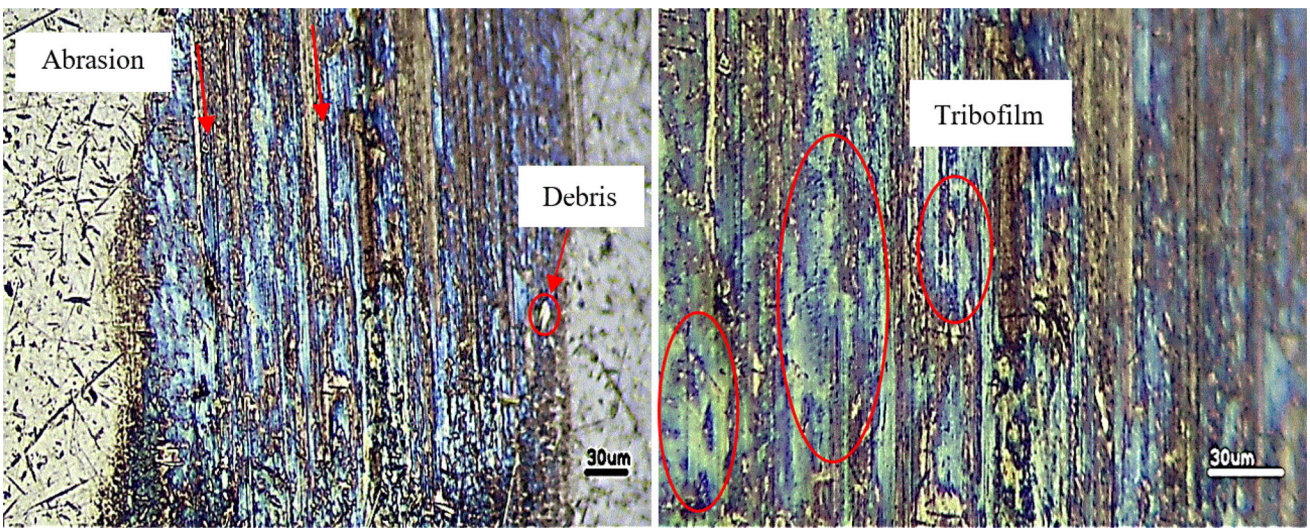

Figure 16. Ball surface after the tribological rest.

A thorough analysis of the ball surface was performed in order to determine the wear mechanisms during the test. Figure 16 shows optical micrographs of the ball surface after the wear test. From this figure, several types of wear have appeared. A strong adhesion of the used oil is noticed on the ball surface. This adhesion leads to the formation of a tribofilm reducing the wear and the friction coefficient. Abrasive wear along the direction of friction was also observed. This type of wear can be caused by the friction between two bodies (ball/sample) or three bodies (ball, sample/debris). This third body is due to wear debris from the ball and/or the sample. If the latter is hard, it will promote abrasive wear to the ball or sample. On the other hand, if the wear debris has a low hardness, it would promote adhesive wear. The most likely wear in this case is three-body abrasive wear with the presence of debris. The latter could be the product of the wear of the ball surface. These results show that the sample is more resistant to wear, which led to abrasion of the ball.

Conclusions

Microstructure, wear and friction of a Ni-Nb-V alloyed manganese steel (HM-NiNbV) under the effect of heat treatment temperature were investigated and compared to those of the same steel as-cat state. The main drawn conclusions are as follows:

- The microstructure, in the as-cast state, of the studied HM-NiNbV consists of an austenitic matrix, alloyed cementite ((Fe, Mn, $Cr)_3C$) precipitated at the grain boundaries and a complex carbide ((Nb, V)C).
- The microstructures, in the heat-treated state, of HM-NiNbV steel are mainly composed of martensite and retained austenite. The rate of the formed martensite increases with increasing of heat treatment temperature, which improves its HRC hardness, wear and friction.
- Application of high load (300 N) in the dry conditions leads to the formation of martensite on the surface of HM-NiNbV steel. Addition of elements (Nb and V) increases the hardenability of the studied steel.
- Friction coefficients of HM-NiNbV steel in lubricated conditions are lower compared to the one carried out in dry conditions. Addition of 5W-40 engine oil promotes the formation of tribofilm reducing the friction of HM-NiNbV steel.
- Application of a high load (60 N) at high temperature (100 °C) in the presence of a lubricating oil promotes a finish polishing improving the surface state of HM-NiNbV steel.

REFERENCES

1. Q. Luo, M. Kitchen, J. Li, W. Li, Y. Li, Experimental investigation on the spalling failure of a railway turnout made from Hadfield steel. Wear **523**(December2022), 204779 (2023). https://doi.org/10.1016/j.wear.2023.204779
2. B. Cheng et al., Materials & Design High strength Hadfield steel produced using laser powder bed fusion of mixed powders. Mater. Des. **231**, 112017 (2023). https://doi.org/10.1016/j.matdes.2023.112017
3. M.K. El Fawkhry, Modified hadfield steel for castings of high and low gouging applications. Int. J. Met. **15**(2), 613–624 (2021). https://doi.org/10.1007/s40962-020-00492-5
4. D. Handayani, V.F. Okhuysen, N. Wagner, Machinability of high Mn steel using tool life criteria. Int. J. Met. **18**(1), 600–607 (2024). https://doi.org/10.1007/s40962-023-01044-3
5. S. Ayadi, A. Hadji, Effect of chemical composition and heat treatments on the microstructure and wear behavior of manganese steel. Int. J. Metacasting (2020). https://doi.org/10.1007/s40962-020-00479-2
6. D. Bańkowski, P.S. Młynarczyk, W. Depczyński, K.C. Bolanowski, The effect of work hardening on the structure and hardness of hadfield steel. Arch. Foundry Eng. (2024). https://doi.org/10.24425/afe.2024.149246
7. J.H. Zhao et al., A quantitative insight into strain hardening behavior of typical Hadfield steel under dynamic load. J. Mater. Res. Technol. **27**(December), 8050–8061 (2023). https://doi.org/10.1016/j.jmrt.2023.11.223
8. J. Nutter, J. Qi, H. Farahani, W.M. Rainforth, S. Van Der Zwaag, Acta materialia in situ TEM observations of the growth of bainitic ferrite in an. Acta Mater. **252**(March), 118924 (2023). https://doi.org/10.1016/j.actamat.2023.118924
9. A. Kozłowska, M. Morawiec, R.H. Petrov, A. Grajcar, Effect of heating and cooling rates on the microstructure of a double soaked medium-manganese Al-alloyed Steel. BHM Berg-und Hüttenmänn. Monatshefte **167**, 538–541 (2022). https://doi.org/10.1007/s00501-022-01289-1
10. M. Hua, C. Chen, Q. Xiangyang, L. Junkui, L. Bo, Effect of rolling temperature on microstructure evolution and mechanical properties of high carbon high manganese steel. J. Mater. Res. Technol. (2022). https://doi.org/10.1016/j.jmrt.2022.09.024
11. Z. Xu, Z. Xia, Y. Xiong, J. Lu, Z. Guo, Multiple morphologies and twin structure generated by a definite growth behavior of grain boundary M 23 C 6 in tempered Fe–15Mn–3Al-0.7C steel. J. Mater. Res. Technol. **28**(April 2023), 774–781 (2024). https://doi.org/10.1016/j.jmrt.2023.12.009

12. J. Wang et al., Effect of rapid tempering at high temperature on microstructure, mechanical properties and stability of retained austenite of medium carbon ultrafine bainitic steel. J. Mater. Res. Technol. **28**, 3144–3154 (2024). https://doi.org/10.1016/j.jmrt.2023.12.238
13. R. Wang, W. Zhang, F. Zhang, H. Fu, The effect of RRA treatment on mechanical properties and wear behavior in vanadium micro-alloyed Hadfield's steel. J. Mater. Res. Technol. **24**, 9884–9896 (2023). https://doi.org/10.1016/j.jmrt.2023.05.156
14. H.R. Jafarian, M. Sabzi, S.H.M. Anijdan, A.R. Eivani, N. Park, The influence of austenitization temperature on microstructural developments, mechanical properties, fracture mode and wear mechanism of Hadfield high manganese steel. J. Mater. Res. Technol. **10**, 819–831 (2020). https://doi.org/10.1016/j.jmrt.2020.12.003
15. S. Ayadi, A. Hadji, Effect of heat treatments on the microstructure and wear resistance of a modified hadfield steel. Metallofiz. Noveishie Tekhnologii **41**(5), 607–620 (2019). https://doi.org/10.15407/mfint.41.05.0607
16. C. Li, X. Deng, L. Huang, Y. Jia, Z. Wang, Effect of temperature on microstructure, properties and sliding wear behavior of low alloy wear-resistant martensitic steel. Wear **442–443**(July 2019), 203125 (2020). https://doi.org/10.1016/j.wear.2019.203125
17. K.F. Rodriguez-galeano, J. Nutter, Y. Azakli, C. Slater, W.M. Rainforth, Influence of Cr and Cr + Nb on the interphase precipitation and mechanical properties of V – Mo microalloyed steels. Mater. Sci. Eng. A **893**(January), 146140 (2024). https://doi.org/10.1016/j.msea.2024.146140
18. S. Ayadi, A. Hadji, K. Hakan, D. Selman, Microstructure and wear behavior of a Cr-Mo-Nb alloyed manganese steel. J. Mater. Res. Technol. **9**(5), 11545–11562 (2020). https://doi.org/10.1016/j.jmrt.2020.08.048
19. D. Zhang et al., Insights into the high magnetic field-induced austenite formation in medium manganese steel. J. Mater. Res. Technol. **25**, 210–221 (2023). https://doi.org/10.1016/j.jmrt.2023.05.189
20. O. Altuntas, A.D. Sciences, N. Defense, Metallurgical and crystallographic analysis of different amounts. Int. J. Metalcasting **17**(2), 1340–1349 (2023). https://doi.org/10.1007/s40962-022-00860-3
21. G. Saha, K. Valtonen, A. Saastamoinen, P. Peura, V. Kuokkala, Impact-abrasive and abrasive wear behavior of low carbon steels with a range of hardness-toughness properties. Wear **450–451**(March), 203263 (2020). https://doi.org/10.1016/j.wear.2020.203263

Publisher's Note Springer Nature remains neutral with regard to jurisdictional claims in published maps and institutional affiliations.

Springer Nature or its licensor (e.g. a society or other partner) holds exclusive rights to this article under a publishing agreement with the author(s) or other rightsholder(s); author self-archiving of the accepted manuscript version of this article is solely governed by the terms of such publishing agreement and applicable law.